ANALYSIS OF DEFORMATION STATES IN HIGH PERFORMANCE FIBRE REINFORCED CONCRETE BENT PLATES

Piotr Smarzewski

Lublin University of Technology, Faculty of Civil Engineering and Architecture,
Department of Civil Engineering, Nadbystrzycka Street 40, 20-618 Lublin, Poland
e-mail: p.smarzewski@pollub.pl

Summary:
The article presents the results of bending tests on reinforced concrete made of high strength concrete with water/cement ratio of 0.2 with addition steel and polypropylene fibres obtained with the non-contact three-dimensional displacement measuring system – ARAMIS. The plates were reinforced with mesh and the variable was the content of fibres in concrete. The results of strains and vertical displacements for characteristic sections in plates P1-P3 were analysed. Examples of the relationship major strains and vertical displacement along section length for P1 were presented. The experiments proved significant influence structural reinforcement combinations on load capacity of plates. The use of polypropylene fibres is effective and increases the performance of the deformed steel fibres in concrete. The cracks in reinforced concrete plates with fibres were much smaller width across than the cracks in the plate reinforced with the reinforcing mesh.

Keywords: reinforced concrete elements, high performance concrete, steel fibres, polypropylene fibres, plates. ARAMIS system.

Introduction

High strength concrete is an increasingly common building material. Its technology has been developed over the years. By adding various additives and admixtures different concrete properties were improved. The addition of fibres allowed to obtain a new composite with a high tensile strength, high resistance to fracture, increased impact resistance and fatigue strength (Brandt 1996, 2008, 2009, Glinicki et al. 2002, Domański, Czkwianianc 2006). Despite the fact that the research on this material last half century, new developments are determined (Walraven 2009, Prisco et al. 2009, Glinicki 2010). The idea that has been recently in the focus is fibre hybridisation. In high strength concrete a few types of fibres are combined in order to define its optimal qualitative and quantitative composition (Banthia, Gupta 2004). Typically, microfibers combine with macrofibres, or similar-sized fibres but different elasticity module. An example is the use of steel or carbon fibres with high elasticity module with polypropylene fibres with low elasticity module. Correctly anchored fibre with high module gains optimal ability strengthen when there are small or medium cracks. On the other hand, fibres with low module obtain full ability strengthen the large cracks. Such a combination of fibres makes a high strength composite with a high range of crack opening.

The experimental tests concern reinforced concrete plates made of high performance concrete reinforced with steel and propylene fibres. Such a concept of a modern composite has a number of enthusiasts (Cucchiara et al. 2004, Chiaia et al. 2009, Fairbairn et al. 2012). The article presents the results and analyses of non-contact, three-dimensional measurements of deformation states of elements obtained using the ARAMIS system.

Preparing HPFRC plates and research using ARAMIS system

Three reinforced concrete plates P1-P3 sized 1000 x 800 x 60 mm were prepared according to recipes M1, M2, and M3 (Table 1). More detailed information concerning element preparation and curing are provided in articles (Smarzewski et al. 2012, Smarzewski 2013).

Table 1. Recipe concrete mixtures

Component	M1 [kg/m^3]	M2 [kg/m^3]	M3 [kg/m^3]
Cement CEM I 52.5R	596	596	596
Granodiorite 2-8 mm	990	990	990
Quartz sand	500	500	500
Condensed microsilica	59.6	59.6	59.6
Superplasticiser	20	20	20
Water	196	196	196
Steel fibres	–	39	78
Polypropylene fibres	–	0.5	0.5

Ready elements covered with random patterns and the laboratory stand with ARAMIS system digital cameras are presented in Fig. 1. The laboratory test were conducted in Zwick/Roell hydraulic press. Prior to the tests the cameras were mounted onto stands and calibrated with a control cross.


Fig. 1. Laboratory stand for testing reinforced concrete plates.

ARAMIS is a system for three-dimensional measuring the states of strains and displacements, analysing, computing and drafting graphical documentation of the results. Its basic element is a measuring sensor with two digital cameras, a stable base for attaching them, release and driving device for cameras, recording device and a high performance computer with software. Clear visuals of the measuring give full understanding of objects' behaviour. The system takes pictures with digital camera and recognises the structure of the measured surfaces. The state of zero displacement is illustrated in the first photography. All pictures are recorded until the element is completely destroyed. The combination of pictures may allow comparing them and calculating the level of displacement and strain. ARAMIS compares the pictures with one another and attributed characteristic area with rectangular plains (with side size of a few pixels) called facets. Then it identifies the areas in the pictures. The measuring range of the sensor is broad and covers the area from 1 mm to 2000 mm. Relative strains are registered in the range from 0.01% up to a few hundred percent. Most functions of the measuring system are controlled by software. ARAMIS system can be used in the following types of tests: defining the strength, nonlinear behaviour tests, creeping, checking verifiable models, e.g. in Finite Elements Method, defining material characteristics, deformation processes and strain calculations (ARAMIS 2011).

Reinforced concrete plates were locally loaded with a centrally located steel plate at constant dislocation of the hydraulic press piston. The research was conducted until the layers in the loaded area of concrete were completely crashed and the cracks in the tensed area were over 5 mm. The recording speed and measurement area were defined for the calculations (Fig. 2).

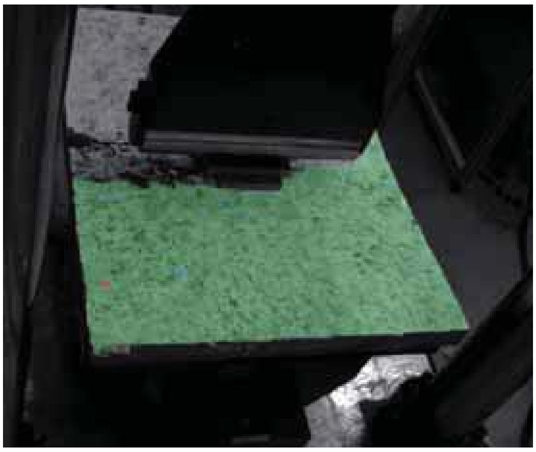

Fig. 2. The measurement area for plate P1 in ARAMIS system

With optical measurement techniques coordinates, displacements and strains will be determined only on the surface of objects. This means that the calculation is limited to local strains, which are tangential to the surface. As additional information perpendicular to the surface is missing, it is not possible to calculate a complete 3D strain tensor. In this case, the calculation of the thickness change is based on the assumption of volume constancy of the material during loading.

Strain is the measure for the deformation of a line element and can be defined as follows:

$$\lambda = \lim_{l \to 0} \left(\frac{l + \Delta l}{l} \right) \tag{1}$$

A strain value can be defined as the function of the stretch ratio λ. The following known functions are frequently used strain measures: technical strain as $\varepsilon^T = f(\lambda) = \lambda - 1$, logarithmic strain as $\varepsilon^L = \varphi = f(\lambda) = \ln(\lambda)$, Green's strain as $\varepsilon^G = f(\lambda) = 1/2(\lambda^2 - 1)$.

In order to quantitatively display the deformation of a surface element, the deformation gradient tensor **F** is introduced. The deformation gradient tensor transforms a line element $d\mathbf{X}$ into the line element dx. In both cases, the line element connects the same material coordinates. Theoretically, it must be an infinitesimal line element. Thus, the deformation gradient tensor is defined as:

$$dx = \mathbf{F} d\mathbf{X} \tag{2}$$

A disadvantage of the deformation gradient tensor is that rotation and stretch are modeled using one matrix only. This can be compensated by splitting the deformation gradient tensor into two tensors: a pure rotation matrix and a pure stretch tensor. The matrix can be decomposed in two different ways. First way is decomposition into rotation **R** and right stretch tensor **U**. Mathematically, the deformation gradient tensor is decomposed as follows:

$$\mathbf{F}=\mathbf{RU} \tag{3}$$

Second way is decomposition into left stretch tensor and rotation. Mathematically, the deformation gradient tensor is decomposed as follows:

$$\mathbf{F}=\mathbf{VR} \tag{4}$$

With the orthogonal rotation matrix the stretch tensor can be computed from the Cuachy Strain tensor:

$$\begin{gathered} \mathbf{C} = \mathbf{F}^T\mathbf{F} = \mathbf{U}^T\mathbf{R}^T\mathbf{R}\mathbf{U} \\ \mathbf{R}^T\mathbf{R} = \mathbf{I} \\ \mathbf{U} = \sqrt{\mathbf{C}} \end{gathered} \tag{5}$$

Values ε_x, ε_y and ε_{xy} can directly be read from the symmetric stretch tensor **U** with the following form:

$$\mathbf{U} = \begin{pmatrix} U_{11} & U_{12} \\ U_{21} & U_{22} \end{pmatrix} = \begin{pmatrix} 1+\varepsilon_x & \varepsilon_{xy} \\ \varepsilon_{xy} & 1+\varepsilon_y \end{pmatrix} \tag{6}$$

The strain measures ε_x, ε_y have the disadvantage of being defined as dependent on the coordinate system. This disadvantage can be eliminated by calculating major and minor strain values. The symmetrical matrix **U** can be transformed to the main diagonal form. The two eigenvalues λ_1 and λ_2 can be calculated as follows:

$$\lambda_{1,2} = 1 + \frac{\varepsilon_x + \varepsilon_y}{2} \pm \sqrt{\left(\frac{\varepsilon_x + \varepsilon_y}{2}\right)^2 - \left(\varepsilon_x \varepsilon_y - \varepsilon_{xy}^2\right)} \tag{7}$$

Frequently, the effective strains are needed. The effective strains according to von Mises and von Tresca are available. The effective strain according to von Mises results from the following formula:

$$\varphi_V = \sqrt{\frac{2}{3}\left(\varphi_1^2 + \varphi_2^2 + \varphi_3^2\right)} \tag{8}$$

As φ_3 is included in the formula, the effective strain is only valid if the volume constancy is valid.

Analysis of tests' results

ARAMIS system has the functionality of drawing graphs of plates response at any point or along a selected section. Fig. 3 illustrates a scheme of plate P1 with characteristic points and sections.

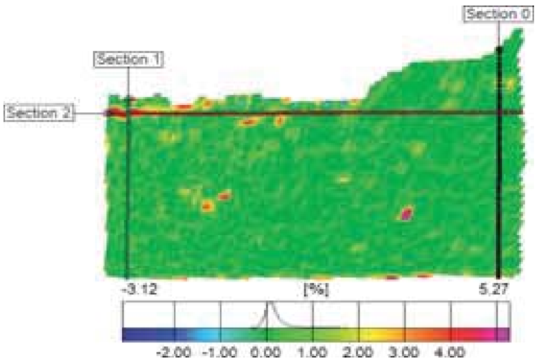

Fig. 3. Example sections selected for plate P1 analysis in ARAMIS

The results of strains and vertical displacements for characteristic sections in the analysed area in plates P1-P3 were presented in a form of images. The images presented in Fig. 4 concern deformation states of plates corresponding to the highest applied load.

P1 – F_{max} = 66.1 kN

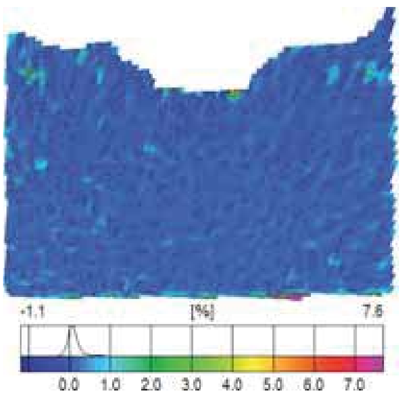

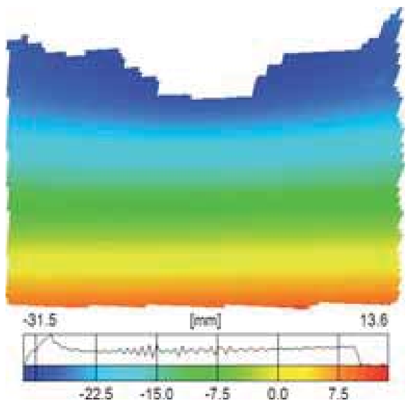

P2 – F_{max} = 72.4 kN

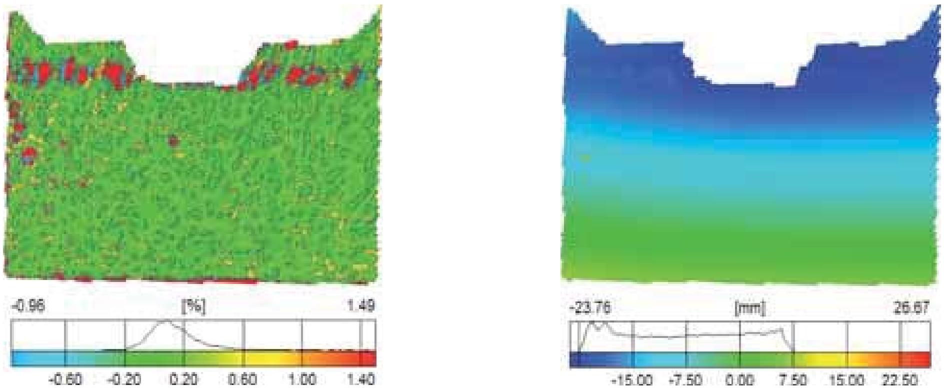

P3 – F_{max} = 72.2 kN

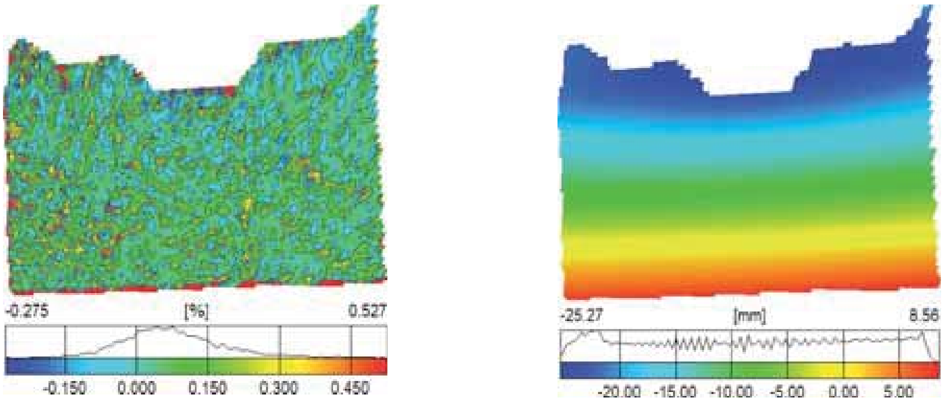

Fig. 4. Images of strains and horizontal displacements of plates at maximum load

Plate P1, without any fibres, was damaged the soonest. Its vertical displacement for maximum strength of 66.1 kN reached the value 31.2 mm. The layer of largest horizontal displacements of 25 to 31.2 mm was 200 mm wide and run centrally across the plate. Maximum values of strains, which appeared at midspan of section 3, were significant and exceeded 3%. They were related to local concrete crushing in the area.

The displacement of plate P2 for maximum load of 72.4 kN reached the value of 32.7 mm. The layer of largest horizontal displacements of 25 to 32.7 mm was reduced to 100 mm. Much smaller strains (1.2%) of elements were observed along all analysed sections. The deformations of 2.8% appeared locally along section 1 in the areas of concrete spalls.

Displacement of plate P3 for maximum value of load equal to 72.2 kN reached the value of 16.2 mm. At the strength value similar to plate P2, local crushing of concrete with fibres appeared. The strains in these areas were the largest, yet they did not exceed 1.2%. Maximum vertical displacements appeared in central layer of 70 mm and reached the value of 12-16.2 mm for the load higher by 18.2% than maximum load for plate P1.

P1 – F_u = 45.4 kN

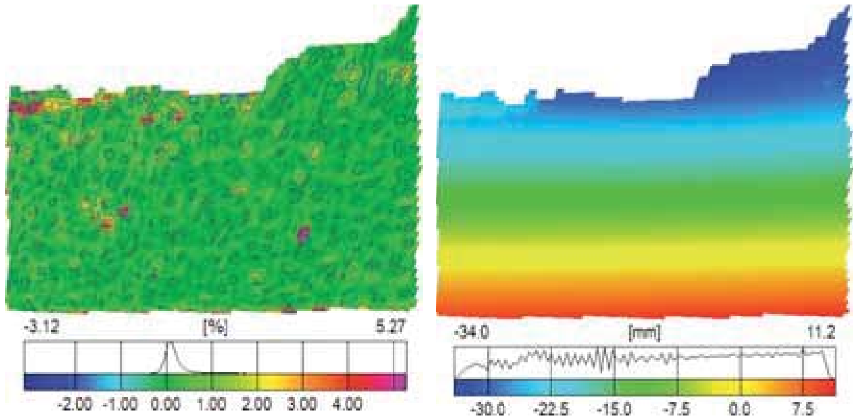

P2 – F_u = 40.8 kN

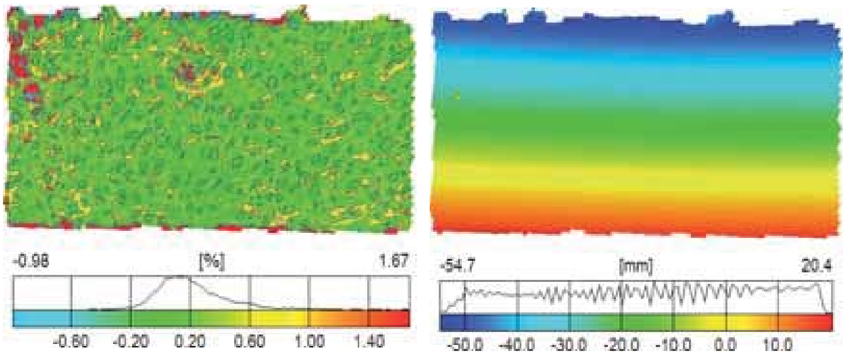

P3 – F_u = 42.1 kN

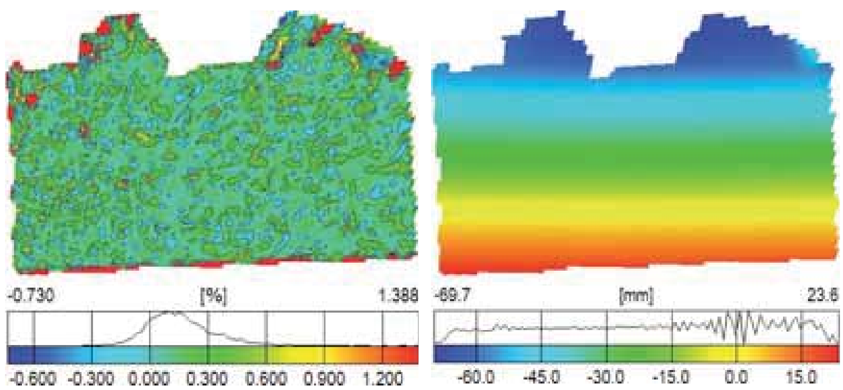

Fig. 5. Images of strains and horizontal displacements of plates at final stage of loading

In the final stage of loading plate P1, the highest strains were recorded along the whole section 2 for the values over 2%. Maximum displacements reached as much as 33.6 mm. In plate P2 strains were usually up to 2% in small fragments. The largest vertical displacements were over twice larger than the displacements in plate P1 and reached 69.8 mm. In P3 with larger share of hybrid fibre reinforcement the strains the compressive fibre concrete layers were larger than in P2 and in longer sections the effects of matrix crushing were observed. The displacements in this case were also significant and reached 56 mm in section 1.

Examples of the relationship major strains and vertical displacement along section length for P1 were presented in Fig. 6.

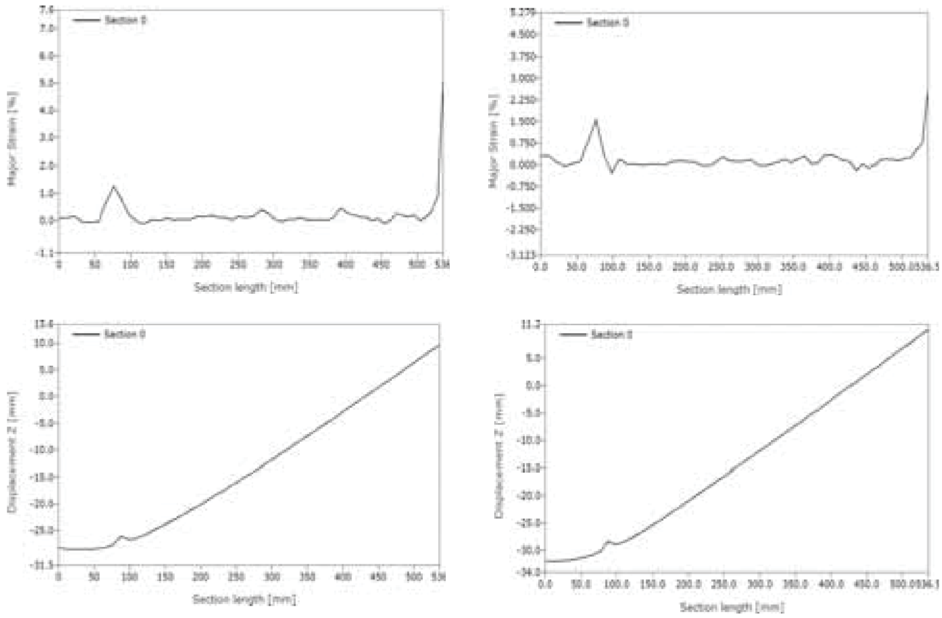

Fig. 6. Sample graphs major strains and vertical displacement along section length for plate P1 at maximum load and final stage of loading

Conclusions

Experimental research proved the correctness of using steel and polypropylene fibres in order to improve the tensile strength of high performance concrete in plate elements. On the basis of the obtained analyses it was stated that 0.5% addition of steel fibres increases the tensile strength of the HPC and stiffness. Moreover, the use of polypropylene fibres, even in small amounts, is effective and increases the performance of the deformed steel fibres in concrete. The cracks in reinforced concrete plates with fibres were much smaller width across than the cracks in the plate reinforced with the reinforcing mesh only. Abrupt energy release was registered in the reinforced concrete plate only. In the plates with fibres instant cracks were observed as a result of bridging fibres. Flexural strength were over 18% for plates with fibres. The failure of reinforced HPC plate with steel fibres in the amount of 1% and polypropylene fibres in the amount of 0.06% was of plastic, gradual and gentle character.

In the most nearest future numerical simulations of failure mechanisms of HPC elements with two kinds of fibres and optimisation of composites are planned.

References:

1. ARAMIS v6.3 (2011), *User Manual - Software*. GOM Optical Measuring Techniques, Germany.
2. Banthia N., Gupta R. (2004), *Hybrid fiber reinforced concrete (HyFRC): fiber synergy in high strength matrices*. Materials and Structures, Vol. 37, 707-716.
3. Brandt A.M. (1996), *Toughness of fibre reinforced cement based materials.* Archives of Civil Engineering, XLII, 4.
4. Brandt A.M. (2008), *Fibre reinforced cement-based (FRC) composites after over 40 years of development in building and civil engineering.* Composite Structures 86, 3-9.
5. Brandt A.M. (2009) *Cement Based Composites: Materials, Mechanical Properties and Performance*. Taylor and Francis. London and New York.
6. Chiaia B., Fantilli A.P., Vallini P. (2009), *Combining fiber-reinforced concrete with traditional reinforcement in tunnel linings.* Engineering Structures 31 1600-1606.
7. Cucchiara C., La Mendola L., Papia M. (2004), *Efectiveness of stirrups and steel fibres as shear reinforcement*. Cement & Concrete Composites 26, 777-786.
8. Domański T., Czkwianianc A. (2006), *Influence of fibre reinforcement on the mechanical parameters of the concrete.* Building Review 6 (in Polish).
9. Fairbairn E.M.R., Toledo Filho R.D., Formagini S., Rosa J.I., Battista R.C. (2012), *Experimental analysis and modeling of ultra high performance fiber reinforced concrete plates*. 1-8.
10. Foster S.J. (2009), *The application of steel-fibres as concrete reinforcement in Australia: from material to structure*. Materials and Structures 42: 1209-1220.
11. Glinicki M.A. (2010), *Concrete with the structural reinforcement*. XXV the Polish Workshops of Work of the Structural Designer, Szczyrk (in Polish).
12. Glinicki M.A., Litorowicz A., Zieliński M. (2002), *Experimental analysis of fracture mode I behaviour of fibre concrete*. Building Materials, No 3, 74-76 (in Polish).
13. Prisco M., Plizzari G., Vandewalle L. (2009), *Fibre reinforced concrete: new design perspectives.* Materials and Structures 42: 1261-1281.
14. Smarzewski P. (2013), *Expermental analysis of high performance fibre reinforced concrete plates.* 1-11 (in press).
15. Smarzewski P., Szwaj M., Szewczak A. (2012), *The analysis of deformation states high strength fibre-reinforced concrete plates in flexural.* Building and Architecture 10, 37-52 (in Polish).
16. Walraven J.C. (2009), *High performance fiber reinforced concrete: progress in knowledge and design codes.* Materials and Structures 42: 1247-1260.

Acknowledgment

This work was financially supported by Ministry of Science and Higher Education within the statutory research number S/15/2013